CHEMISTRY
A EUROPEAN JOURNAL

DOI: 10.1002/chem.200700665

Structure–Fluorescence Contrast Relationship in Cyanine DNA Intercalators: Toward Rational Dye Design

Alexandre Fürstenberg,[a] Todor G. Deligeorgiev,[b] Nikolai I. Gadjev,[b] Aleksey A. Vasilev,[b] and Eric Vauthey*[a]

Abstract: The fluorescence enhancement mechanisms of a series of DNA stains of the oxazole yellow (YO) family have been investigated in detail using steady-state and ultrafast time-resolved fluorescence spectroscopy. The strong increase in the fluorescence quantum yield of these dyes upon DNA binding is shown to originate from the inhibition of two distinct processes: 1) isomerisation through large-amplitude motion that non-radiatively deactivates the excited state within a few picoseconds and 2) formation of weakly emitting H-dimers. As the H-dimers are not totally non-fluorescent, their formation is less efficient than isomerisation as a fluorescent contrast mechanism. The propensity of the dyes to form H-dimers and thus to reduce their fluorescence contrast upon DNA binding is shown to depend on several of their structural parameters, such as their monomeric (YO) or homodimeric (YOYO) nature, their substitution and their electric charge. Moreover, these parameters also have a substantial influence on the affinity of the dyes for DNA and on the ensuing sensitivity for DNA detection. The results give new insight into the development and optimisation of fluorescent DNA probes with the highest contrast.

Keywords: aggregation · cyanines · DNA recognition · fluorescent probes · intercalation · photoisomerization

Introduction

Rapid and highly sensitive detection of nucleic acid sequences is crucial for medical diagnosis and for understanding biomolecular mechanisms.[1] Interest in non-radioactive detection of nucleic acids has led to the search for stains that are stable under gel electrophoretic conditions.[2,3] A breakthrough in this area was made in the 1990s with the discovery of the oxazole yellow (YO) and thiazole orange (TO) dye families and their homodimeric relatives YOYO and TOTO.[4,5] These dyes have very high extinction coefficients ($\approx 10^5\ cm^{-1}\,M^{-1}$), are virtually non-fluorescent when free in solution and form highly fluorescent and stable intercalation complexes with double-stranded DNA.[6] These attractive characteristics enabled DNA to be detected for the first time at a sensitivity comparable to that of radioactive probes, but without the danger inherent in radioactivity.[7]

Although some sequence specificity that might lead to inhomogeneous staining has been demonstrated for both TOTO and, to a lesser extent, YOYO,[8–10] these cyanines and some derivatives have been used as general DNA stains in numerous DNA detection and quantitation assays,[11] such as the polymerase chain reaction,[12,13] DNA staining and fragment sizing,[14–18] DNA damage detection,[19,20] flow cytometry,[16,21,22] evaluation of biological activity,[23,24] DNA imaging[25–28] and DNA photocleavage.[29–31] YO and TO have also been covalently linked to oligonucleotides and inserted into peptide nucleic acids constructs, which become fluorescent upon hybridisation of the light-up probe to a specific complementary strand.[32–38]

The origin of the very high contrast in emission between the free and the bound form of the dyes has long been thought to be due to an ultrafast decay of the excited state of the free form through a large-amplitude torsional motion around the monomethine bond connecting the benzoxazole, benzothiazole and quinoline moieties, respectively.[39,40] This isomerisation mechanism is blocked upon intercalation of the dyes into DNA and, as a consequence, they light-up by three orders of magnitude. Very recently, however, we have shown that, in aqueous solution, YOYO derivatives form in-

[a] A. Fürstenberg, Prof. Dr. E. Vauthey
Physical Chemistry Department, University of Geneva
Quai Ernest-Ansermet 30, 1211 Genève 4 (Switzerland)
Fax: (+41) 22-379-6518
E-mail: eric.vauthey@chiphy.unige.ch

[b] Prof. Dr. T. G. Deligeorgiev, Dr. N. I. Gadjev, Dr. A. A. Vasilev
Faculty of Chemistry, University of Sofia
James-Bourchier Avenue 1, 1126 Sofia (Bulgaria)

Supporting information for this article is available on the WWW under http://www.chemeurj.org/ or from the author.

tramolecular face-to-face, and thus poorly fluorescent, H-aggregates[39,41] and that disruption of these aggregates upon intercalation also contributes significantly to the fluorescence enhancement of these homodimeric dyes.[41]

Yoctomole detection of YOYO-stained DNA with a high-sensitivity laser-induced fluorescence detector has been reported[15] and picogram quantities of double-stranded DNA can be detected on gels in the presence of micromolar free dye concentrations;[42] however, there is still a need for developing more efficient dyes that enable facile detection of trace amounts of DNA, and new dyes with improved characteristics are proposed regularly.[6] One evident way to achieve better sensitivity with the oxazole yellow dye family would be to improve the contrast between the free and the bound forms of the dyes. However, the fluorescence quantum yield of the bound dyes (on the order of 0.4–0.5)[40,41] can be enhanced by a factor of ≈ 2 at the most, which means that a reduction in the fluorescence quantum yield of the free dyes has also to be sought. A thorough understanding of the factors that influence 1) the large-amplitude torsional motion and 2) aggregation would thus be very helpful for designing improved dyes rationally. Driven by previous results which suggested that free homodimeric dyes that aggregate have an enhanced, although very low, fluorescence quantum yield with respect to dyes that do not aggregate,[41] we have therefore investigated a series of monomeric (YO) and homodimeric (YOYO) derivatives of oxazole yellow by time-resolved fluorescence and steady-state absorption and fluorescence spectroscopies.[41,43] We will show below that aggregation also operates at low concentration with the monomeric dyes, that this process is controlled mainly by the charge and the nature of the substituents of the dyes, and that maximum contrast between free and bound forms would be reached with dyes for which aggregation can be minimised and isomerisation is the fastest.

Results and Discussion

Homodimeric dyes—intramolecular H-aggregation: The absorption spectrum in organic solvents of the YOYO derivatives investigated displays a single maximum at approximately 490 nm with a shoulder around 465 nm ascribed to a vibronic transition,[39] whereas in aqueous solution it is characterised by two maxima around 460 and 485 nm (Figure 1; Figure S1 in the Supporting Information). The blue-shifted 460 nm peak is characteristic of dimeric H-type aggregate formation and can be associated with the transition to the upper excitonic state of such an H-dimer,[41,44] whereas the 485 nm peak is representative of the non-aggregated dye population. Since the relative intensity of the two bands does not depend on concentration (data not shown),[39] aggregation must be intramolecular: it takes place between the two chromophoric units of the molecule and is strongly favoured by the pre-organisation induced by the linker, which removes the serendipitous diffusion step in dilute solution.

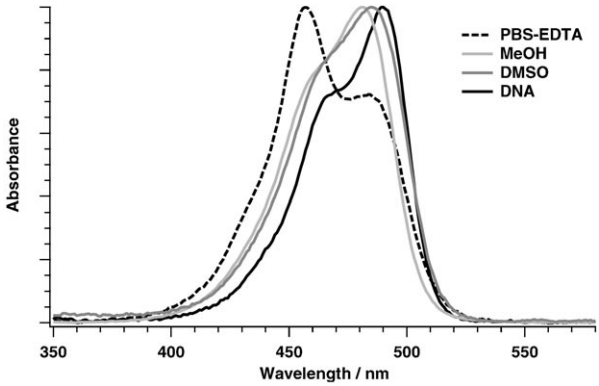

Figure 1. Intensity-normalised absorption spectra of 1 μM YOYO-1 in various solvents and in DNA.

It is known that cyanine dyes undergo aggregation,[44–47] a phenomenon that is mainly due to a strong hydrophobic effect. Aggregation dramatically changes the photophysical properties of the dyes in solution compared to the monomeric species, in particular the absorption and fluorescence band shape and position (Figure 2). The dye molecules may aggregate parallel to each other, face-to-face (plane-to-plane stacking; so-called H-aggregates),[48] or in a parallel end-to-end arrangement (head-to-tail stacking; so-called J-aggregates).[49,50] The photophysical properties of these aggregates have been explained by Kasha and Davydov in terms of molecular exciton coupling theory.[51,52] In a dimeric aggregate, the excitonic coupling between the two dye molecules results in a splitting of the excited state. In H-aggregates, the transition to the upper excitonic state is allowed, but not that to

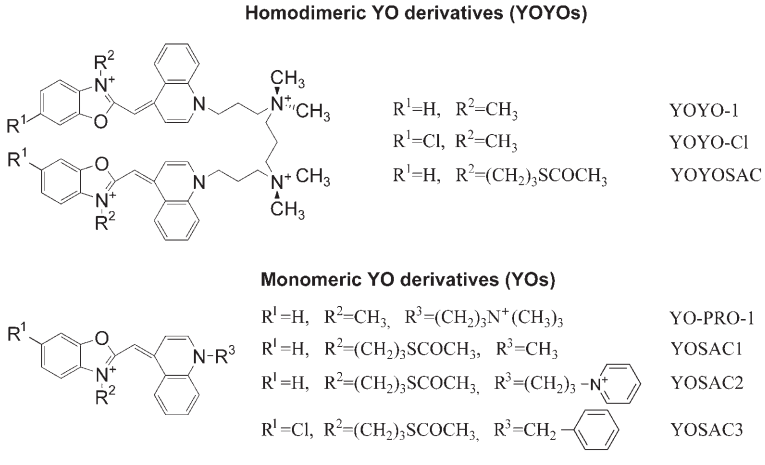

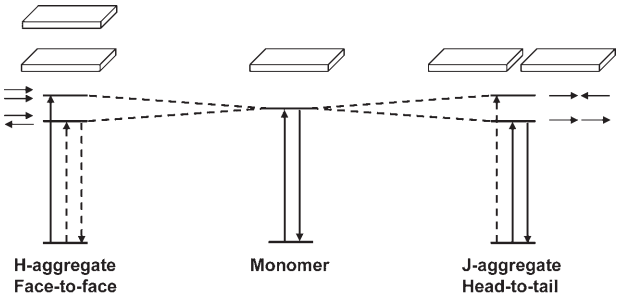

Figure 2. Schematic representation of the effect of excitonic interaction on the energy levels of aggregated and non-aggregated molecules depending on their relative spatial arrangement (small arrows represent transition dipole moments).

the lower state. This results in a blue shift of the absorption spectrum and usually in a non-fluorescent aggregate because of very fast internal conversion from the upper to the lower "dark" excitonic state. In J-aggregates, the situation is reversed: the electronic transition to the upper excitonic state is forbidden, whereas it is strongly allowed to the lower excitonic state, resulting in a highly fluorescent aggregate.

Further evidence of aggregation of the YOYO derivatives in aqueous solution and even to some extent in organic solvents (since the process is intramolecular) is found in the very broad fluorescence emission spectra (Figure 3; Figure S2 in the Supporting Information), which are not mirror images of the absorption (whereas in organic solvents and in DNA, they are), and in the wavelength dependence of the fluorescence excitation spectra (Figure 4).[41] The excitation spectrum is dominated by the contribution of the H-dimers at long emission wavelengths and by that of the monomers at short emission wavelengths.

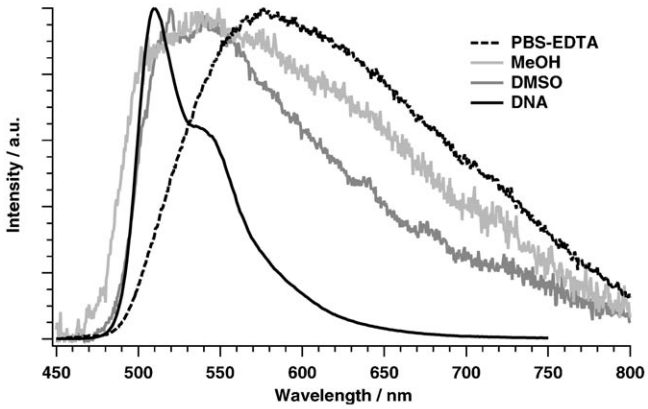

Figure 3. Intensity-normalised fluorescence spectra of 1 μM YOYO-1 in various solvents and in DNA.

Upon intercalation into DNA, the dimeric aggregates are disrupted and all the spectral features of the dyes inside DNA are very similar to those in organic solvents, except that the fluorescence intensities and lifetimes are strongly enhanced (Tables 1 and 2) because of the constrictive DNA environment which inhibits torsional non-radiative deactivation of the excited state. The suppression of the excitonic interaction is due not so much to the distance between the two chromophores in DNA as to their quasi-orthogonal relative orientation (NMR measurements of TOTO-1 bound to DNA indicate a dihedral angle 83° between the chromophoric units).[53] Indeed, it was demonstrated that the interaction between the chromophoric units is sufficient to allow high enough excitation energy to hop between the two chromophores within a few picoseconds.[39,41,54]

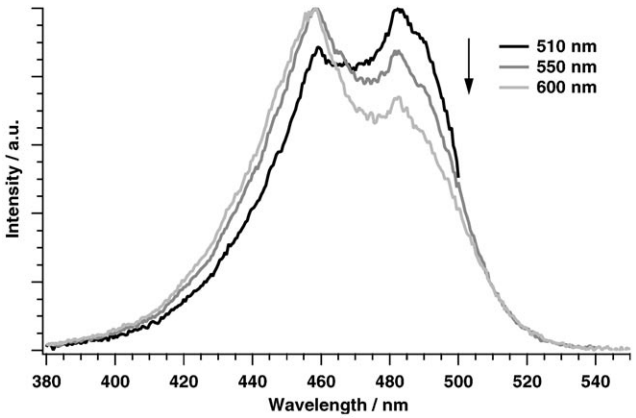

Figure 4. Intensity-normalised excitation spectra of 1 μM YOYOSAC in aqueous buffer solution monitored at various emission wavelengths.

Table 1. Fluorescence quantum yield Φ_{fl} of the dyes in aqueous buffer solution and in the presence of 50 base pair equivalents of DNA.

Dye	Φ_{fl}(free) × 10^4	Φ_{fl}(bound)	Contrast
YOYO-1	11	0.46	410
YOYOSAC	14	0.41	290
YOYO-Cl	38	0.52	130
YO-PRO-1	2.4	0.42	1660
YOSAC1	5.3	0.35	620
YOSAC2	3.6	0.41	1060
YOSAC3[a]	9.7	0.61	590
TOSAC3	6.4	ND[b]	ND

[a] In distilled water. [b] ND: not determined.

Table 2. Time constants related to nanosecond decay components of the fluorescence of the dyes in aqueous buffer solution and in the presence of 50 base pair equivalents of DNA.[a]

Dye	τ(free) [ns]	τ(bound) [ns]
YOYO-1	1.1	1.9 (0.36)/4.1 (0.64)
YOYOSAC	1.2	1.8 (0.30)/3.9 (0.70)
YOYO-Cl	1.6	2.3 (0.29)/4.4 (0.71)
YO-PRO-1	2.6	1.9 (0.45)/4.1 (0.55)
YOSAC1	0.4 (0.37)/3.2 (0.63)	2.2 (0.68)/4.8 (0.32)
YOSAC2	2.8	2.3 (0.36)/4.3 (0.64)
YOSAC3[b]	0.9 (0.55)/3.2 (0.45)	2.5 (0.35)/4.5 (0.65)

[a] Relative amplitudes differing from 1 are indicated in brackets. For better comparison, the total amplitude of these ns components was set to 1. [b] In distilled water.

Monomeric dyes—intermolecular H-aggregation: In contrast to the YOYO derivatives, the absorption spectra of the different monomeric YO derivatives studied do not exhibit major changes on going from organic solvents to aqueous solution (Figure 5; Figure S3 in the Supporting Information).

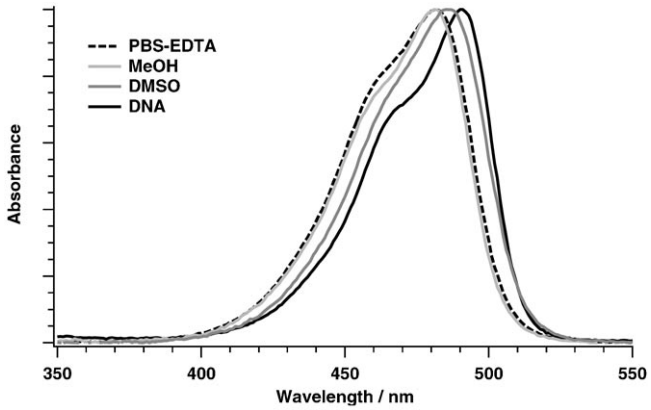

Figure 5. Intensity-normalised absorption spectra of YO-PRO-1 in various organic solvents and in DNA.

As with non-aggregated homodimeric dyes, a single maximum at 490 nm and a shoulder around 460 nm characterise the spectra. In water, however, the height of the shoulder at 460 nm increases with rising concentrations of YOSAC1 and YOSAC3 in the 1–50 μM range, suggesting that these two dyes now undergo intermolecular aggregation (Figure 6). At higher ionic strength (PBS–EDTA: that is, aqueous buffer solution containing 137 mM NaCl; PBS = phosphate buffer saline, EDTA = ethylenediaminetetraacetate) or 200 μM dye concentration, this effect is even more pronounced and aggregation becomes noticeable with YOSAC2 also. The similarity to the spectra obtained with the homodimeric dyes and the position of the aggregate band suggest strongly that the aggregates formed here are dimeric and not higher order H-aggregates.[44] Dimerisation of cyanine dyes is a well-documented phenomenon.[44,45] Higher order aggregates would have an absorption band shifted more to the blue. The H-dimer association constant (Table 3) was estimated from the dependence of the absorbance of the monomer absorption band on the total dye concentration, as suggested by Harris and Hobbs.[55]

Aggregation is further confirmed by the shape of the fluorescence spectra of all the monomeric YO derivatives investigated, which depend on their concentration in aqueous solution (Figure 7). Both the non-aggregated form, the spectrum of which is a mirror image of the absorption spectrum with its maximum at 505 nm, and the aggregated form, with a broad and red-shifted spectrum, contribute to the fluorescence spectra; the contribution of the latter rises with increasing dye and thus H-dimer concentration. Although no sign of aggregation can be found in the absorption spectrum of YO-PRO-1 (Figure 6), its fluorescence excitation (Figure 8) and emission (Figure 7) spectra display a wavelength dependence, revealing that it also forms dimeric H-aggregates, albeit with lower propensity than YOSAC1, YOSAC2 or YOSAC3, since they can be detected only with

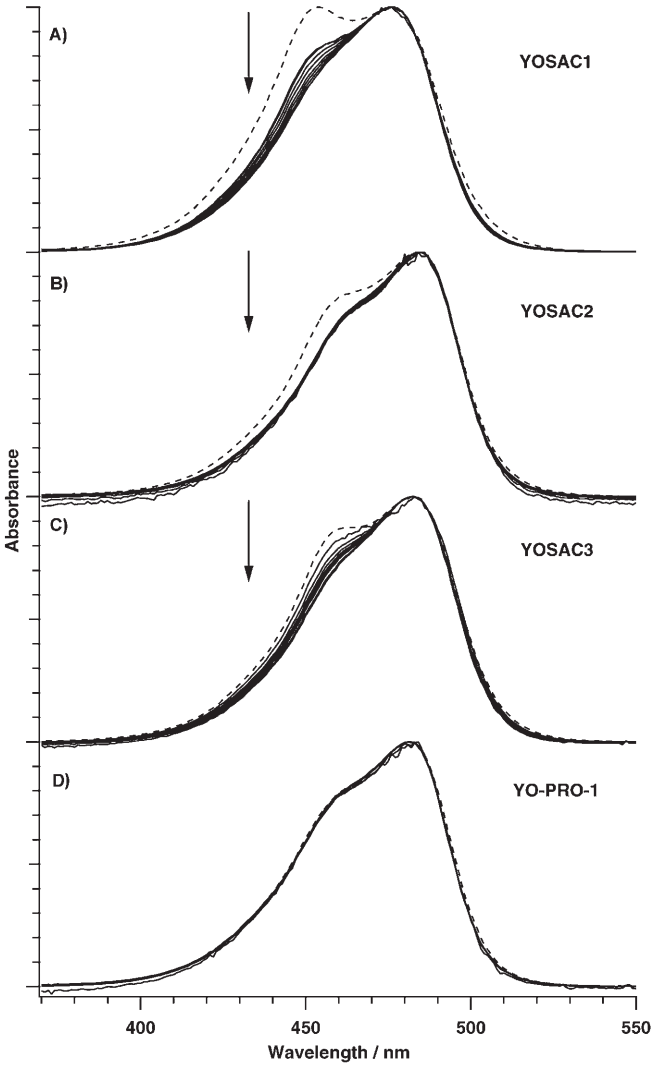

Figure 6. Intensity-normalised absorption spectra of 50 μM A) YOSAC1, B) YOSAC2, C) YOSAC3, and D) YO-PRO-1 in water diluted to A) 3.1 μM, B) 4.7 μM, C) 0.8 μM and D) 6.2 μM (solid lines). The broken lines correspond to a concentration of 200 μM in aqueous buffer solution except for YOSAC3, for which the solvent is water.

Table 3. H-Dimer formation constant K_{HD}, affinity constant K for DNA, EC_{50} values and cooperativity parameter s (Hill slope).

Dye	K_{HD} [M^{-1}]	K [M]	$EC_{50} \pm SD$ [μM]	$s \pm SD$
YOYO-1	ND[b]	4.6×10^7	20 ± 1	1.36 ± 0.07
YOYOSAC	ND	1.2×10^7	12 ± 1	1.29 ± 0.13
YOYO-Cl	ND	1.8×10^7	8 ± 1	1.7 ± 0.2
YO-PRO-1	ND	4.5×10^5	35 ± 2	1.10 ± 0.04
YOSAC1	2.3×10^3	2.7×10^5	118 ± 7	1.03 ± 0.05
YOSAC2	ND	2.4×10^5	47 ± 2	1.17 ± 0.06
YOSAC3[a]	1.5×10^3	ND	290 ± 40	0.99 ± 0.07
TOSAC3	4.0×10^3	ND	ND	ND

[a] In distilled water. [b] ND: not determined.

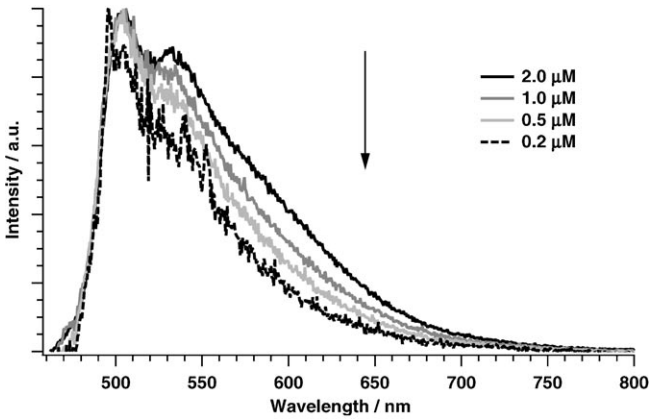

Figure 7. Intensity-normalised fluorescence spectra of YO-PRO-1 in aqueous buffer solution at various dye concentrations.

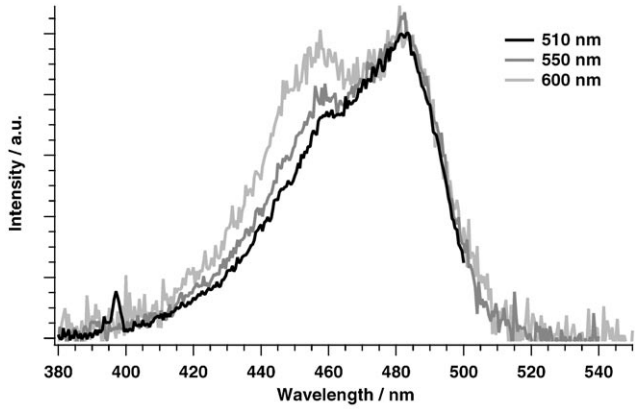

Figure 8. Intensity-normalised excitation spectra of 1 μM YO-PRO-1 in aqueous buffer solution monitored at various emission wavelengths.

the high sensitivity of fluorescence spectroscopy. As with the YOYO dyes, the fluorescence spectra in organic solvents are much narrower and closer to the mirror image of the absorption (Figure 9), indicating that aggregation is most efficient in aqueous solution.

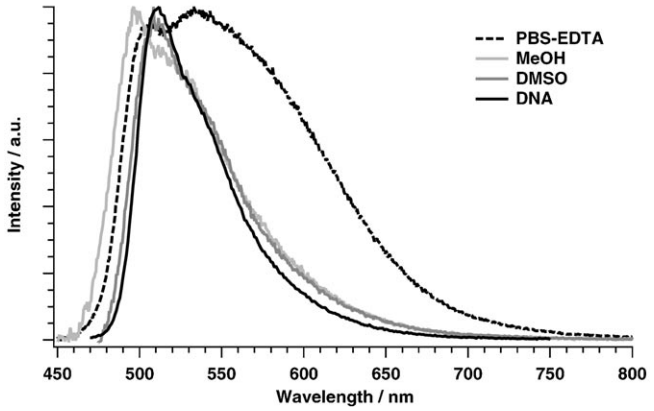

Figure 9. Intensity-normalised fluorescence spectra of YOSAC1 in various solvents and in DNA.

The fluorescence dynamics of the free dyes further supports aggregation in aqueous solution (a detailed investigation of the dynamics will be described elsewhere).[56] Most of the fluorescence decays within the first 20 ps, during which the dynamics is dominated by isomerisation of the non-aggregated dyes, that is, large-amplitude torsional motion governed by solvent friction. In aqueous solution, residual fluorescence with time constants in the nanosecond timescale (Table 2) is however observed additionally (Figure S8 in the Supporting Information), whereas in organic solvents, in which no H-dimers are detected, the fluorescence intensity reaches zero after a period ranging from a few picoseconds to a few tens of picoseconds, depending on solvent viscosity (Figure 10).[56] The amplitude spectrum associated with these nanosecond components observed in aqueous solution is representative of the steady-state fluorescence spectrum of the H-dimer population with a broad band and a maximum in the 550–600 nm region (Figure 11). Assuming that these H-dimers have a similar fluorescence

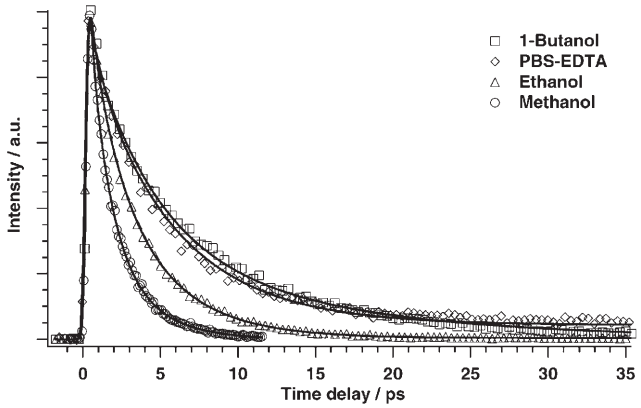

Figure 10. Fluorescence dynamics of YOSAC1 in various solvents measured at the fluorescence maximum (510 nm in organic solvents, 550 nm in water).

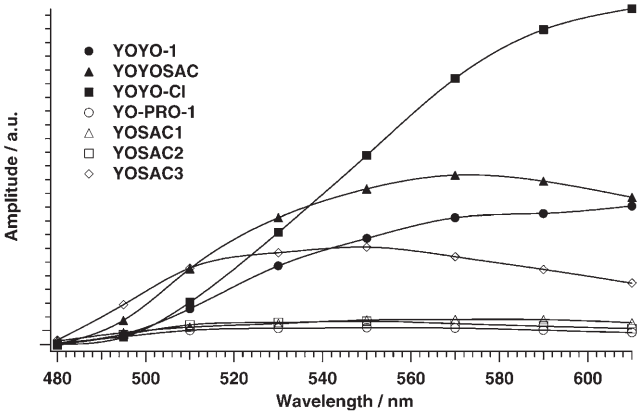

Figure 11. Decay-associated amplitude spectra of the nanosecond component ascribed to the aggregate fluorescence.

quantum yield, the area of these spectra is thus a direct measure of the H-dimer population (all experiments were performed at the same total chromophore concentration). Its amplitude follows the trend YOYO-Cl $\gg$ YOYOSAC $>$ YOYO-1 $\gg$ YOSAC3 $\gg$ YOSAC1 $\approx$ YOSAC2 $>$ YO-PRO-1, confirming that the homodimeric dyes aggregate more efficiently than the monomeric dyes and that, as observed by others, the introduction of a chlorine atom in the 4,4′-position of the benzoxazole ring (YOYO-Cl and YOSAC3) favours aggregation.[44,57]

Upon intercalation into DNA, the H-dimers are disrupted, the fluorescence spectra become mirror images of the absorption (Figure S4 in the Supporting Information) and, as with the homodimeric dyes, the fluorescence intensities and lifetimes increase strongly (Tables 1 and 2; Figure S11 in the Supporting Information).

Effect of aggregation on the fluorescence contrast: It is striking that the fluorescence quantum yields of the free dyes in aqueous solution (Table 1) are directly correlated with the amplitude of the nanosecond decay component of the fluorescence and thus with the aggregated dye population: the more efficient the H-dimer formation, the higher the fluorescence quantum yield.

As explained above, both the aggregated and non-aggregated dye populations contribute to the fluorescence spectrum and thus to the fluorescence quantum yield. The radiative rate constant of the non-aggregated dyes in water can be estimated from that of the DNA-bound form, after correction for the difference in refractive indices,[58] to be about $(0.7–1)\times10^8\,s^{-1}$. The non-aggregated dyes thus have a high radiative rate constant, but contribute very little to emission since their excited state is very short-lived (<10 ps in water). On the other hand, the aggregated population has a much lower radiative rate constant, but is much longer-lived: its contribution cannot be neglected, since a broadening of the fluorescence spectra originating from the aggregates is evident in water compared to other environments. It is estimated that the fluorescence quantum yields of the unbound homodimeric dyes would be three to seven times lower if the formation of H-dimers could be prevented in water.[41] This indicates that aggregation is not as efficient as isomerisation as a fluorescence contrast mechanism, at least in the case of the dyes investigated here, and thus that it should be avoided in order to optimise the fluorescence contrast.

Influence of electric charge and substitution on aggregation: At the concentrations investigated, only YOSAC1 and YOSAC3 were found to have concentration-dependent absorption spectra in pure water, but not YO-PRO-1 or YOSAC2 (aggregation could, however, be detected by fluorescence, which is a more sensitive technique; see above). The same behaviour was observed in aqueous buffer solution at an ionic strength close to that of intracellular conditions, except for YOSAC2, for which aggregation could also be monitored by absorption spectroscopy. At very high salt concentrations (6 M NaCl), YO-PRO-1 was also shown to aggregate efficiently enough to induce changes in the absorption spectrum.[39] YOSAC1 and YOSAC3 have one net positive charge, whereas YO-PRO-1 and YOSAC2 have two. The amplitude of the nanosecond components in the fluorescence decay is higher with the singly charged than with the doubly charged dyes. This correlates with the fluorescence quantum yields, which are higher with the free form of YOSAC1 and YOSAC3 than with YO-PRO-1 or YOSAC2. Overall, this indicates that aggregation is more efficient with the monocationic monomeric dyes for which the electrostatic repulsion is weaker than with the dicationic derivatives.

The situation is slightly different with the homodimeric dyes. They have four net positive charges, but the aggregation mechanism is different. The spacer linking the two chromophoric units of the homodimers pre-organises the molecule in such a way that the rate-limiting diffusion step for H-dimer formation is removed and that aggregation becomes very efficient, as shown by the higher amplitude of the nanosecond decay component of the fluorescence. As a result, the fluorescence quantum yield is higher with the homodimeric YOYO than with the monomeric YO dyes.

The efficiency of H-dimer formation does not depend only on the net electric charge of the dyes, which causes electrostatic repulsion between the chromophores, but is also dictated by hydrophobic and π–π stacking effects arising from aromatic or long aliphatic substituents. YO-PRO-1 is the dye which aggregates the least in our study. It is monomeric (no pre-organisation), is doubly charged and has a short aliphatic substituent on the quinoline ring. Replacing its substituent by a charged aromatic moiety (YOSAC2) or by an uncharged short aliphatic side chain (YOSAC1) leads to a rise in the fluorescence quantum yield due to enhanced aggregation. Combining both effects by introducing an uncharged aromatic substituent (YOSAC3) causes the dyes to aggregate even more; that is, the fluorescence quantum yield increases further. Interestingly, depending on the ionic strength of the aqueous solution, YOSAC3 is also able to form J-aggregates, indicating multiple possible stacking interactions.[56] The influence of aromatic substituents on aggregation is further confirmed by preliminary investigations of a monocationic benzyl-substituted TO derivative (TOSAC3) (Figure S5 in the Supporting Information). Despite its more efficient aggregation, this dye is less fluorescent than YOSAC3, because the sulfur atom lowers the energy barrier for rotation around the monomethine bond;[10] this enables faster torsion and thus reduces the excited-state lifetime (Figure S8 in the Supporting Information) and the fluorescence quantum yield. Similarly, TO-PRO-1 was shown to be less fluorescent than its oxygen-containing analogue YO-PRO-1.[40] Since the isomerisation is essentially barrier-free and controlled purely by friction,[56] optimisation of this structural parameter in terms of fluorescence quantum yield of the unbound dye seems difficult. Overall, these results reveal that the number of electric charges and the nature of the substituents on the quinoline

ring regulate the aggregation behaviour of the dyes, while the nature of the heteroatom influences to some extent the rate of the non-radiative deactivation.

Influence of electric charge on DNA detection sensitivity: Not only does the net electric charge of the dyes affect their propensity to aggregate, but it is also expected to influence their binding affinity to DNA, since DNA is a highly negatively charged polymer.[59] Intrinsic binding constants are usually measured by titrating a constant amount of dye with DNA and following changes in the absorption spectrum.[60,61] Assuming the existence of only two species (in view of the presence of an isosbestic point), the fractions of free and bound dyes are thus obtained (Figure 12) and binding constants are extracted using the McGhee and von Hippel equation, which takes into account the multiple possible overlapping binding sites of the DNA strands.[62] In good agreement with the literature,[60] we find with this approach that the homodimeric dyes have higher affinity for DNA than the monomeric ones (binding constants of $10^7\,M^{-1}$ versus $10^5\,M^{-1}$, Table 3). However, contrary to intuition and to the single order of magnitude variation observed by Petty et al. between the monocationic TO and the dicationic TO-PRO-1 at similar ionic strengths,[60] no significant difference in DNA affinity among the monomeric derivatives is observed here, suggesting that the predominant parameter which dictates the binding affinity is the stacking interaction between the chromophores and the base pairs rather than electrostatics.

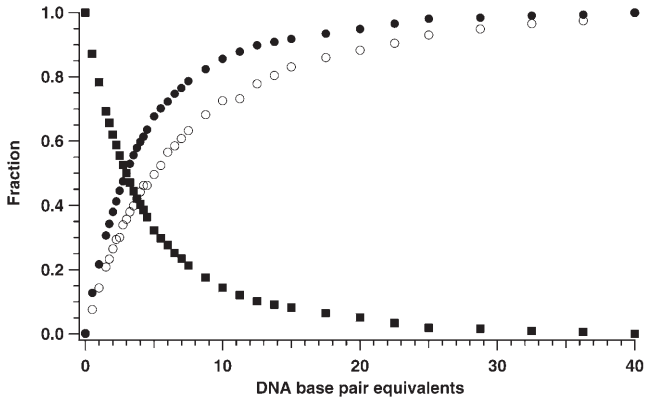

Figure 12. Fraction of free (squares) and bound (circles) YO-PRO-1 determined by absorption (filled symbols) and by fluorescence (open symbols) spectroscopy, assuming a two-state model.

However, the fluorescence intensity at the fluorescence maximum increases more slowly upon addition of DNA than the bound dye fraction determined from the changes in the absorption spectrum (Figure 12). The same behaviour has been reported for TO-PRO-1.[60] In other words, the fact that the absorption spectrum of a given dye molecule changes from the apparently free to the apparently bound form is not a sufficient condition for the same molecule to switch from a non-fluorescent to a fluorescent state, which also means that more than only two species (quasi non-emitting free and strongly emitting bound dyes) contribute to the absorption spectrum. Accordingly, dose–response curves monitoring the fluorescence intensity—the important parameter for DNA detection—versus the DNA concentration at constant (1 μM) dye concentration clearly show that, compared to the homodimeric dyes, the fluorescence increase with rising DNA content is delayed with the dicationic monomeric derivatives and even further delayed with the monocationic monomeric dyes (Figure 13). The dose–response curves were analysed with the Hill equation (Table 3). In agreement with previous studies,[54,60] no significant cooperativity effect for the binding of the dyes has been found. The observation of a Hill slope greater than one with the homodimers can be explained by the increase in steepness of the dose–response curves when the dye concentration is higher than the dissociation constant value (zone B regime according to Straus and Goldstein's nomenclature).[63,64] The trends in the absolute detectability and, as the slopes are all similar in this case, in the EC_{50} value (the DNA concentration at which the fluorescence intensity reaches half its maximum value) are important for DNA detection assays, since the detection sensitivity will be dictated in the end by the ability of the dye to switch to its fluorescent state at a DNA concentration that is as low as possible. Rather than having no effect as suggested by the results obtained by monitoring the absorption spectrum, high electric charge therefore seems to be beneficial, since it favours the formation of the fluorescent dye species.

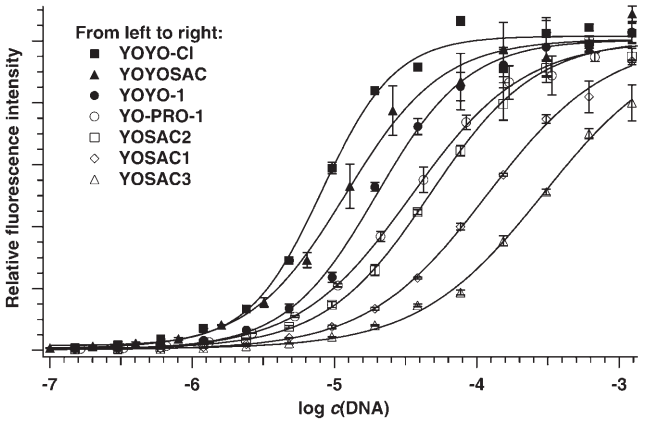

Figure 13. Fluorescence intensity at the maximum wavelength compared to the maximum fluorescence intensity as a function of DNA base concentration. Dye concentration is 1 μM. Data points are normalised to the maximum plateau value determined.

It is worth noting that the binding constants of the monomers are two orders of magnitude greater than the constants of H-dimer formation, confirming that, in the presence of DNA, binding to DNA is thermodynamically preferred over self-association and is expected to be nearly quantitative.

Conclusion

Our investigations demonstrate that two important mechanisms regulate the fluorescence contrast between the free and DNA-bound forms of both monomeric and homodimeric derivatives of the YO family: 1) isomerisation through large-amplitude torsional motion in the excited state and 2) aggregation of the dyes into H-dimers. The best fluorescence contrast would be reached with dyes for which isomerisation is the fastest and aggregation is minimised. The isomerisation rate is dictated mainly by the nature of the heteroatom in the benzoxazole or benzothiazole ring and the friction from the solvent, and thus cannot be influenced strongly, although TO derivatives seem to isomerise faster than YO derivatives. The aggregation behaviour can be tuned, however, and here we have investigated mainly the parameters that control aggregation. It turns out that aggregation is less efficient with highly charged dyes and is favoured by the presence of aromatic substituents and covalent links between two dyes (homodimeric dyes). Highly cationic dyes were further shown to light up at lower DNA concentrations than monocationic ones. Overall, the ideal dye with the highest possible contrast should thus be monomeric, highly charged, and have side chains that do not induce aggregation.

Experimental Section

Samples: All dyes were iodide salts synthesised according to the literature.[41,65,66] Ethanol and dimethyl sulfoxide (DMSO) were purchased from Fluka, methanol from Acros Organics, 1-butanol from Merck, phosphate buffer saline (PBS, composition: NaCl 137 mM, KCl 26.8 mM, Na_2HPO_4 8.1 mM, KH_2PO_4 1.5 mM, ref. D8537) and double-stranded salmon sperm DNA from Sigma, and EDTA disodium salt dihydrate from AppliChem. All compounds were of the highest commercially available grade and used without further purification. The absence of impurities in the solvents was checked by exciting the pure solvents at 400 nm and looking for any emission not attributable to Raman scattering. Stock solutions (1 or 2 mM) of the dyes were prepared in DMSO and stored in the dark. DNA (1 mg mL^{-1}) stock solutions in twice-distilled water were stored at −20 °C. All samples were freshly prepared from the stock solutions. For steady-state and time-correlated single-photon counting measurements, the dye concentration was of the order of 1–2 μM, and for fluorescence up-conversion experiments it was about 100–200 μM. Unless specified, all measurements with the bound dyes were performed with a DNA base pair/dye ratio of 50:1 and experiments with all dyes were performed in PBS containing EDTA (1 mM) except with YOSAC3, which was handled in distilled water to avoid J-aggregate formation. An average extinction coefficient of 13 200 cm^{-1} M^{-1} per base pair was used to determine DNA concentrations.[67] All experiments were performed between 18 and 22 °C.

Steady-state measurements: Absorption spectra were recorded on a Cary 50 spectrophotometer in a 1 cm quartz cell. Fluorescence emission and excitation spectra were measured on a Cary Eclipse fluorimeter (5 nm slit) in a 1 cm quartz cell. Fluorescence spectra were recorded upon excitation at 440 nm and corrected for the wavelength-dependent sensitivity of the detection. Quantum yield measurements were performed at 1–2 μM dye concentration against fluorescein in NaOH at pH 13 ($\Phi_{fl}=0.95$)[68] or free YOYO-1 ($\Phi_{fl}=0.0011$).[40] Relative errors in the quantum yield values are estimated to ±10 %.

Titration experiments: DNA was added stepwise from a stock solution (0.5 mM) to a constant amount of dye (1–2 μM) in PBS–EDTA in a quartz cuvette, and the mixture was allowed to equilibrate for 1 min. Absorption and/or fluorescence spectra were recorded subsequently until no further change in the absorption was detected. Both kinds of spectra were corrected for dilution afterwards.

Determination of the DNA binding constants: To measure the affinity of the dyes for DNA, the following equilibrium was considered: dye + DNA↔dye•DNA. The experiment relied on the changes in the absorption spectrum of the free and bound forms of the dyes; the determination of their fractions was therefore necessary. The dye was first added to the buffer, providing the reference for the unbound dye. This dye solution was then titrated with DNA and the reference spectrum for the bound dye was obtained after sufficient DNA had been added for no further variation in the absorption spectrum to be detected. Using these reference spectra, the free and bound dye fractions were determined by expressing all intermediate absorption spectra by a linear combination of the two reference spectra [Eqs. (1) and (2)].[60]

$$A = A_f[\mathrm{dye}]_f + A_b[\mathrm{dye}]_b \quad (1)$$

$$[\mathrm{dye}]_{total} = [\mathrm{dye}]_f + [\mathrm{dye}]_b \quad (2)$$

Considering that only the free and bound dye species contribute to the absorption, the measured absorbance A at any wavelength is the sum of the absorbance of the free dyes A_f and of the bound dyes A_b. Since the total dye concentration $[\mathrm{dye}]_{total}$ was kept constant during the titration, the free $[\mathrm{dye}]_f$ and bound dye $[\mathrm{dye}]_b$ concentrations could be determined by mass balance. To confer more stability to the calculation, the whole spectra were reproduced by fitting this linear combination to the measured spectra and by the use of a non-linear least-squares algorithm (MATLAB, The MathWorks Inc.).

Once the free and bound fractions of the dyes were known, a Scatchard plot of $r/[\mathrm{dye}]_f$ versus r was constructed, in which $r=[\mathrm{dye}]_b/c_{total}(\mathrm{DNA})$ is the average number of bound dyes per base pair and $c_{total}(\mathrm{DNA})$ the total DNA concentration. The excluded site model of McGhee and von Hippel was applied to find the binding constant K and the site exclusion parameter n by using a non-linear least-squares fitting procedure (MATLAB, The MathWorks Inc.) [Eq. (3)].[62]

$$\frac{r}{[\mathrm{dye}]_f} = K(1-nr)\left[\frac{1-nr}{1-(n-1)r}\right]^{n-1} \quad (3)$$

Values of between 15 and 80 % bound ligand were used to provide the most accurate estimates of K and n.[60] The error in K and n is estimated to be ±50 %.

Determination of the H-dimer association constants: The absorption spectrum of the dye (50 μM) was recorded. The sample was then diluted and its spectrum monitored successively down to a concentration of a few micromolar. The H-dimer association constant K_{HD} was estimated by using equation [Eq. (4)] proposed by Harris and Hobbs,[55] in which A_{na} is the absorbance at the maximum of the non-aggregated dye band (which, to a first approximation, is attributed to absorption of the non-aggregated dyes only!), ε_{na} the extinction coefficient of the non-aggregated species, l the optical path length and $c_{total}(\mathrm{dye})$ the total dye concentration.

$$A_{na} = \frac{K_{HD}}{2}\varepsilon_{na}^2 l^2 \frac{c_{total}(\mathrm{dye})}{A_{na}} - \frac{K_{HD}}{2}\varepsilon_{na} l \quad (4)$$

A plot of A_{na} versus $c_{total}(\mathrm{dye})/A_{na}$ should yield a straight line the intercept and slope of which allow K_{HD} and ε_{na} to be determined. It was confirmed that the approximation that the absorbance at the maximum of the non-aggregated dye band is due only to the non-aggregated dyes is

reasonable, since the H-dimer concentration was low even at the highest total dye concentration (50 μM versus K_{HD} in the 200–700 μM range). The error in K_{HD} is large and thus only the order of magnitude should be considered.

Dose–response fluorescence titration: Solutions were prepared directly in disposable plastic cuvettes (1 cm) in which the fluorescence intensity was measured. DNA was added to PBS–EDTA (1.9 mL) in the first cuvette, which contained the highest DNA concentration in the experiment (≈1 mM). The other cuvettes containing lower DNA concentrations were prepared by diluting the first solution in series. Once all the solutions with the various DNA concentrations had been prepared, a constant dye concentration (1 μM) was added to all the cuvettes, which were stirred and left for 5 min so that the solutions could equilibrate. For each cuvette, the fluorescence intensity at 510 nm was then read three times. The error bars represent the standard deviation over these three measurements. Dose–response curves were analysed using the Hill equation [Eq. (5)] for describing the DNA concentration-dependent fluorescence intensity $I(c)$, in which I_{min} and I_{max} are the minimal and maximal fluorescence plateau values, respectively, c the DNA concentration, s the Hill slope (or cooperativity parameter) and the EC_{50} the value of the DNA concentration at which 50% of the maximum fluorescence intensity is achieved.

$$I(c) = I_{min} + \frac{(I_{max} - I_{min})}{\left(1 + \frac{EC_{50}}{c}\right)^{s}} \quad (5)$$

Time-resolved fluorescence measurements: Excited-state lifetime measurements on the nanosecond timescale were carried out by the time-correlated single-photon counting (TCSPC) technique as previously described.[41] Excitation was performed at a repetition rate of 40 MHz with ≈60 ps pulses generated by a laser diode at 395 nm (Picoquant model LDH-P-C-400B). The full width at half maximum (FWHM) of the instrument response function (IRF) was around 200 ps. All measurements were performed in a quartz cell (1 cm). The accuracy of the lifetimes is approximately 0.1 ns.

Excited-state dynamics on shorter timescales was investigated by the fluorescence up-conversion technique. The experimental set-up has been described in detail elsewhere.[69] Excitation was achieved at 400 nm with the frequency-doubled output of a Kerr lens mode-locked Ti:sapphire laser (Tsunami, Spectra-Physics). The output pulses centred at 800 nm had a duration of 100 fs and a repetition rate of 82 MHz. The polarisation of the pump beam was set at the magic angle relative to that of the gate pulses at 800 nm. Experiments were carried out in a rotating cell (1 mm). The FWHM of the IRF was approximately 280 fs. No significant degradation of the samples was observed after the measurements. The measured data were analysed by iterative reconvolution of a Gaussian IRF with a sum of one Gaussian and several exponential functions according to standard procedures.[56] The accuracy of the lifetimes and of the amplitudes obtained by this method is estimated to approximately 10%.

Acknowledgement

This work was supported by the Fonds National Suisse de la Recherche Scientifique through project no. 200020-115942. The authors thank Prof. Stefan Matile (University of Geneva) for bringing the Straus and Goldstein paper to their attention.

[1] C.-Y. Zhang, H.-C. Yeh, M. T. Kuroki, T.-H. Wang, *Nat. Mater.* **2005**, *4*, 826–831.
[2] A. N. Glazer, K. Peck, R. A. Mathies, *Proc. Natl. Acad. Sci. USA* **1990**, *87*, 3851–3855.
[3] H. S. Rye, M. A. Quesada, K. Peck, R. A. Mathies, A. N. Glazer, *Nucleic Acids Res.* **1991**, *19*, 327–333.
[4] H. S. Rye, S. Yue, D. E. Wemmer, M. A. Quesada, R. P. Haugland, R. A. Mathies, A. N. Glazer, *Nucleic Acids Res.* **1992**, *20*, 2803–2812.
[5] L. G. Lee, C. H. Chen, L. A. Chiu, *Cytometry* **1986**, *7*, 508–517.
[6] R. P. Haugland, *The Handbook—A Guide to Fluorescent Probes and Labeling Technologies*, 10th ed., Molecular Probes, Invitrogen, Eugene (OR), **2005**.
[7] P. Selvin, *Science* **1992**, *257*, 885–886.
[8] L. F. Hansen, L. K. Jensen, J. P. Jacobsen, *Nucleic Acids Res.* **1996**, *24*, 859–867.
[9] J. Bunkenborg, M. M. Stidsen, J. P. Jacobsen, *Bioconjugate Chem.* **1999**, *10*, 824–831.
[10] F. Johansen, J. P. Jacobsen, *J. Biomol. Struct. Dyn.* **1998**, *16*, 205–222.
[11] H. Ihmels, D. Otto, *Top. Curr. Chem.* **2005**, *258*, 161–204.
[12] H. E. Schwartz, K. J. Ulfelder, *Anal. Chem.* **1992**, *64*, 1737–1740.
[13] F. Pellissier, C. M. Glogowski, S. F. Heinemann, M. Ballivet, V. Ossipow, *Anal. Biochem.* **2006**, *350*, 310–312.
[14] L. J. Kricka, *Ann. Clin. Biochem.* **2002**, *39*, 114–129.
[15] D. Figeys, E. Arriaga, A. Renborg, N. J. Dovichi, *J. Chromatogr. A* **1994**, *669*, 205–216.
[16] X. Yan, W. K. Grace, T. M. Yoshida, R. C. Habbersett, N. Velappan, J. H. Jett, R. A. Keller, B. L. Marrone, *Anal. Chem.* **1999**, *71*, 5470–5480.
[17] H. S. Rye, S. Yue, M. A. Quesada, R. P. Haugland, R. A. Mathies, A. N. Glazer, *Methods Enzymol.* **1993**, *217*, 414–431.
[18] H. Zhu, S. M. Clark, S. C. Benson, H. S. Rye, A. N. Glazer, R. A. Mathies, *Anal. Chem.* **1994**, *66*, 1941–1948.
[19] K. Elmendorff-Dreikorn, C. Chauvin, H. Slor, J. Kutzner, R. Batel, W. E. G. Muller, H. C. Schroder, *Cell. Mol. Biol.* **1999**, *45*, 211–218.
[20] K. R. Rogers, A. Apostol, S. J. Madsen, C. W. Spencer, *Anal. Chem.* **1999**, *71*, 4423–4426.
[21] J. T. Petty, M. E. Johnson, P. M. Goodwin, J. C. Martin, J. H. Jett, R. A. Keller, *Anal. Chem.* **1995**, *67*, 1755–1761.
[22] G. T. Hirons, J. J. Fawcett, H. A. Crissman, *Cytometry* **1994**, *15*, 129–140.
[23] R. A. Blaheta, B. Kronenberger, D. Woitaschek, S. Weber, M. Scholz, H. Schuldes, A. Encke, B. H. Markus, *J. Immunol. Methods* **1998**, *211*, 159–169.
[24] S.-J. Choi, F. C. Szoka, *Anal. Biochem.* **2000**, *281*, 95–97.
[25] T. T. Perkins, D. E. Smith, S. Chu, *Science* **1994**, *264*, 819–822.
[26] T. T. Perkins, S. R. Quake, D. E. Smith, S. Chu, *Science* **1994**, *264*, 822–826.
[27] C. Kanony, B. Aakerman, E. Tuite, *J. Am. Chem. Soc.* **2001**, *123*, 7985–7995.
[28] A. E. Cohen, W. E. Moerner, *Phys. Rev. Lett.* **2007**, *98*, 116001–116004.
[29] B. Aakerman, E. Tuite, *Nucleic Acids Res.* **1996**, *24*, 1080–1090.
[30] M. Thompson, N. W. Woodbury, *Biochemistry* **2000**, *39*, 4327–4338.
[31] K. P. Mahon, Jr., R. F. Ortiz-Meoz, E. G. Prestwich, S. O. Kelley, *Chem. Commun.* **2003**, 1956–1957.
[32] T. Ishiguro, J. Saitoh, H. Yawata, M. Otsuka, T. Inoue, Y. Sugiura, *Nucleic Acids Res.* **1996**, *24*, 4992–4997.
[33] R. Lartia, U. Asseline, *Chem. Eur. J.* **2006**, *12*, 2270–2281.
[34] N. Svanvik, A. Stahlberg, U. Sehlstedt, R. Sjoback, M. Kubista, *Anal. Biochem.* **2000**, *287*, 179–182.
[35] N. Svanvik, G. Westman, D. Wang, M. Kubista, *Anal. Biochem.* **2000**, *281*, 26–35.
[36] D. V. Jarikote, N. Krebs, S. Tannert, B. Roeder, O. Seitz, *Chem. Eur. J.* **2007**, *13*, 300–310.
[37] O. Koehler, D. V. Jarikote, O. Seitz, *ChemBioChem* **2005**, *6*, 69–77.
[38] O. Koehler, D. V. Jarikote, O. Seitz, *Chem. Commun.* **2004**, 2674–2675.
[39] C. Carlsson, A. Larsson, M. Jonsson, B. Albinsson, B. Norden, *J. Phys. Chem.* **1994**, *98*, 10313–10321.
[40] T. L. Netzel, K. Nafisi, M. Zhao, J. R. Lenhard, I. Johnson, *J. Phys. Chem.* **1995**, *99*, 17936–17947.

[41] A. Fürstenberg, M. D. Julliard, T. G. Deligeorgiev, N. I. Gadjev, A. A. Vasilev, E. Vauthey, *J. Am. Chem. Soc.* **2006**, *128*, 7661–7669.
[42] A. N. Glazer, H. S. Rye, *Nature* **1992**, *359*, 859–861.
[43] A. Fürstenberg, M. D. Julliard, T. G. Deligeorgiev, N. I. Gadjev, A. A. Vassilev, E. Vauthey in *Femtochemistry VII: Fundamental Ultrafast Processes in Chemistry, Physics, and Biology* (Eds.: A. W. Castleman, Jr., M. L. Kimble), Elsevier, Amsterdam, **2006**, pp. 391–395.
[44] D. Takahashi, H. Oda, T. Izumi, R. Hirohashi, *Dyes Pigm.* **2005**, *66*, 1–6.
[45] A. Mishra, R. K. Behera, P. K. Behera, B. K. Mishra, G. B. Behera, *Chem. Rev.* **2000**, *100*, 1973–2011.
[46] K. C. Hannah, B. A. Armitage, *Acc. Chem. Res.* **2004**, *37*, 845–853.
[47] R. F. Khairutdinov, N. Serpone, *J. Phys. Chem. B* **1997**, *101*, 2602–2610.
[48] L. G. S. Brooker, F. L. White, D. W. Heseltine, G. H. Keyes, S. G. Dent, E. J. Van Lare, *J. Photogr. Sci.* **1953**, *1*, 173–183.
[49] E. E. Jelley, *Nature* **1936**, *138*, 1009–1010.
[50] G. Scheibe, *Angew. Chem.* **1936**, *48*, 563.
[51] M. Kasha, H. R. Rawls, M. A. El-Bayoumi, *Pure Appl. Chem.* **1965**, *11*, 371–392.
[52] A. S. Davydov, *Theory of Molecular Excitons*, Plenum, New York, **1971**.
[53] H. P. Spielmann, D. E. Wemmer, J. P. Jacobsen, *Biochemistry* **1995**, *34*, 8542–8553.
[54] A. Larsson, C. Carlsson, M. Jonsson, B. Albinsson, *J. Am. Chem. Soc.* **1994**, *116*, 8459–8465.
[55] J. T. Harris, Jr., M. E. Hobbs, *J. Am. Chem. Soc.* **1954**, *76*, 1419–1422.
[56] A. Fürstenberg, E. Vauthey, unpublished results.
[57] M. Iwaska, K. Higashinaka, T. Tanaka, *J. Soc. Photogr. Sci. Technol. Jpn.* **1995**, *58*, 361–367.
[58] S. J. Strickler, R. A. Berg, *J. Chem. Phys.* **1962**, *37*, 814–822.
[59] L. Stryer, *Biochemistry*, 4th ed., Freeman, New York, **1995**.
[60] J. T. Petty, J. A. Bordelon, M. E. Robertson, *J. Phys. Chem. B* **2000**, *104*, 7221–7227.
[61] A. Granzhan, H. Ihmels, G. Viola, *J. Am. Chem. Soc.* **2007**, *129*, 1254–1267.
[62] J. D. McGhee, P. H. von Hippel, *J. Mol. Biol.* **1974**, *86*, 469–489.
[63] B. K. Shoichet, *J. Med. Chem.* **2006**, *49*, 7274–7277.
[64] O. H. Straus, A. Goldstein, *J. Gen. Physiol.* **1943**, *26*, 559–585.
[65] T. Deligeorgiev, N. Gadjev, A. Vasilev, K.-H. Drexhage, S. M. Yarmoluk, *Dyes Pigm.* **2006**, *70*, 185–191.
[66] N. I. Gadjev, T. G. Deligeorgiev, I. Timcheva, V. Maximova, *Dyes Pigm.* **2003**, *57*, 161–164.
[67] J. Sambrook, E. F. Fritsch, T. Maniatis, *Molecular Cloning—A Laboratory Manual*, 2nd ed., Cold Spring Harbor, New York, **1989**.
[68] J. R. Lakowicz, *Principles of Fluorescence Spectroscopy*, 2nd ed., Kluwer, New York, **1999**.
[69] A. Morandeira, L. Engeli, E. Vauthey, *J. Phys. Chem. A* **2002**, *106*, 4833–4837.

Received: May 2, 2007
Published online: July 19, 2007

